Supplemental Information for CrRLK1L receptor-like kinases HERCULES RECEPTOR KINASE 1 and ANJEA are female determinants of pollen tube reception

Sergio Galindo-Trigo[1], Noel Blanco-Touriñán[2], Thomas A. DeFalco[3,4], Eloise S. Wells[1], Julie E Gray[5], Cyril Zipfel[3,4], Lisa M Smith[1*]

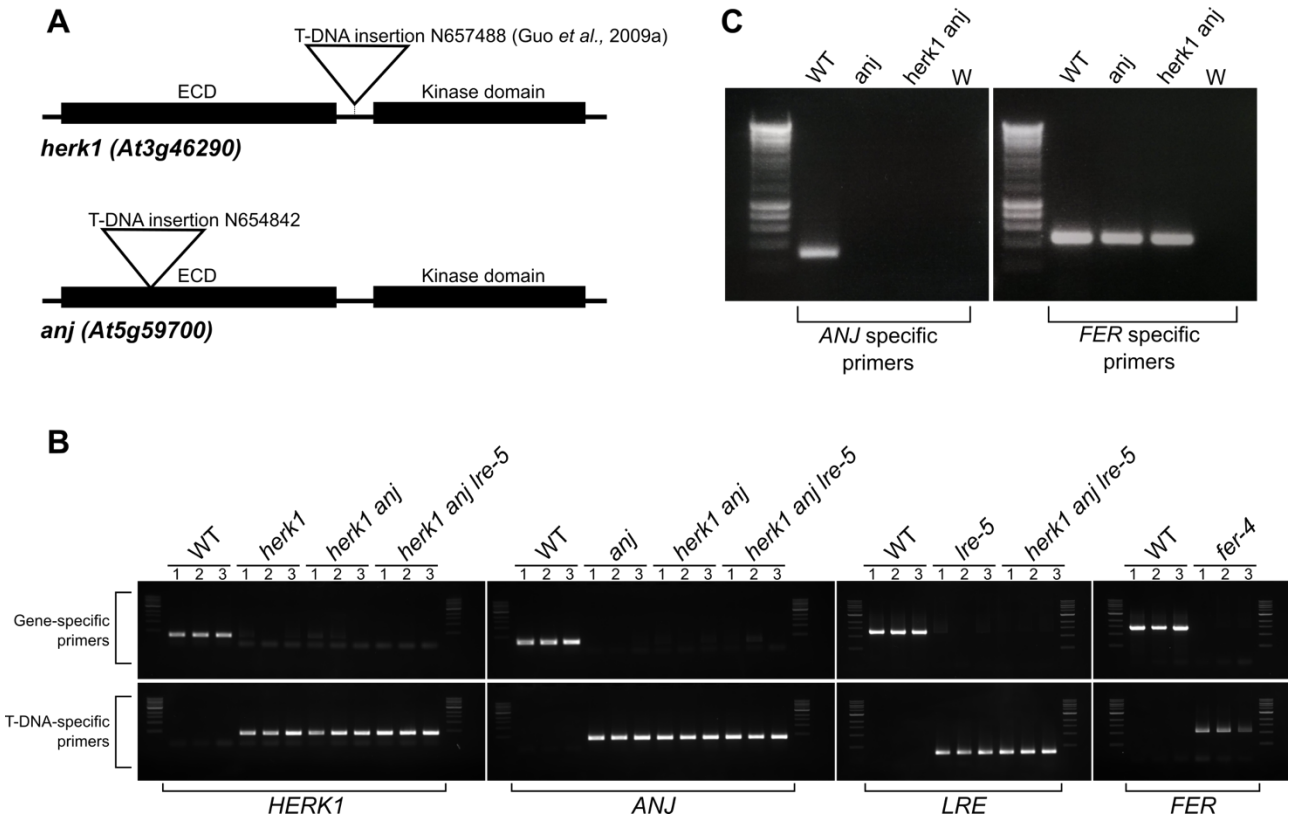

Figure S1. Confirmation of *ANJEA* gene expression knock out and genotyping of T-DNA lines used in this study. (A) Diagram of the domain organisation of *HERK1* and *ANJEA* and T-DNA insertion sites in the lines used in this study, *herk1-1* and *anj-1*. (B) Genotyping PCRs to verify homozygosity in the lines used in this study. DNA from three independent seedlings per line was analysed. (C) RT-PCR analysis of *ANJ* gene expression in wild-type, *anj* and *herk1 anj* plants. RNA was extracted from multiple inflorescences from five plants per line. W indicates a water control with no cDNA added to the RT-PCR reaction.

Figure S2. Growth comparison of WT and *herk1 anj* plants. (A-B) Representative wild-type plants at 10 and 21 days old. (C-D) Representative *herk1 anj* plants at 10 and 21 days old. (E-F) Representative *fer-4* plants at 10 and 21 days old. (G) Representative wild-type and *herk1 anj* plants (left and right, respectively) at 5 weeks old. Scale bars = 1.5 cm.

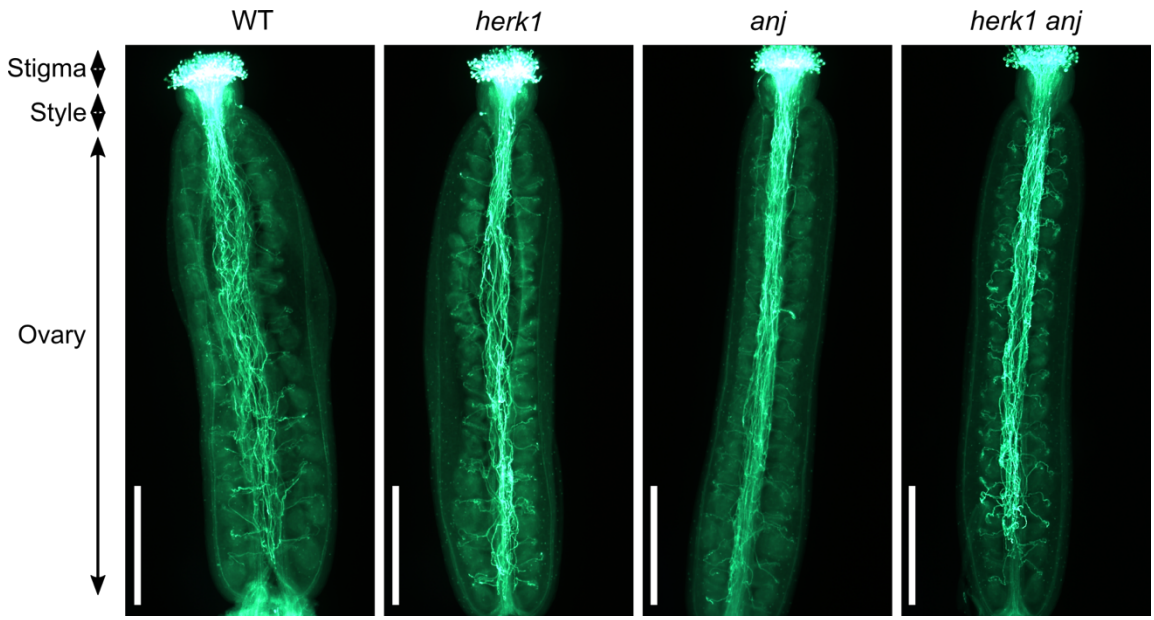

Figure S3. Pollen tube growth and targeting of ovules is not altered in *herk1 anj* plants. Aniline blue staining of pollen tubes in self-pollinated stage 16 flowers in wild-type, *herk1*, *anj* and *herk1 anj* plants. Scale bars = 500 µm.

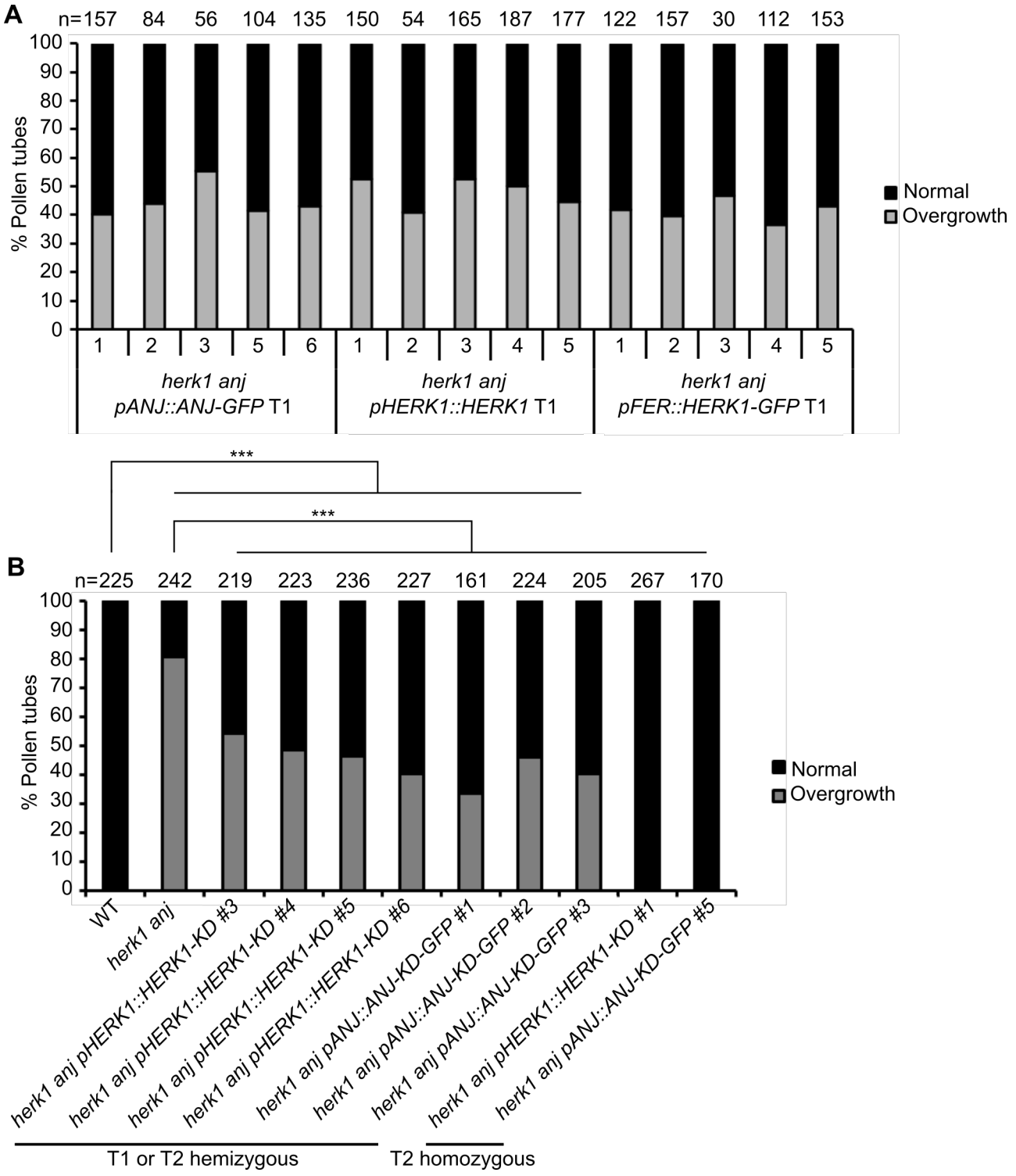

Figure S4. The *herk1 anj* defect in pollen tube reception can be complemented by expression of *HERK1*, *ANJ*, *HERK1-KD* and *ANJ-KD* constructs. (A) Percentage of pollen tubes with normal reception at the female gametophyte (black bars) and displaying overgrowth (grey bars) in siliques of five independent T1 *herk1 anj* plants transformed with *pANJ::ANJ-GFP*, *pHERK1::HERK1* and *pHERK1::HERK1-GFP*. Pollen tube reception was scored for ovules in at least three siliques per line. (B) Percentage of pollen tubes with normal reception at the female

gametophyte (black bars) and displaying overgrowth (grey bars) in WT, *herk1 anj* plants and at least 4 independent lines of *herk1 anj* transformed with *pHERK1::HERK1-KD* or *pANJ::ANJ-KD-GFP* from generations T1 or T2. Pollen tube reception was scored for ovules in at least three siliques per line. *** $p<0.001$ (χ-square tests).

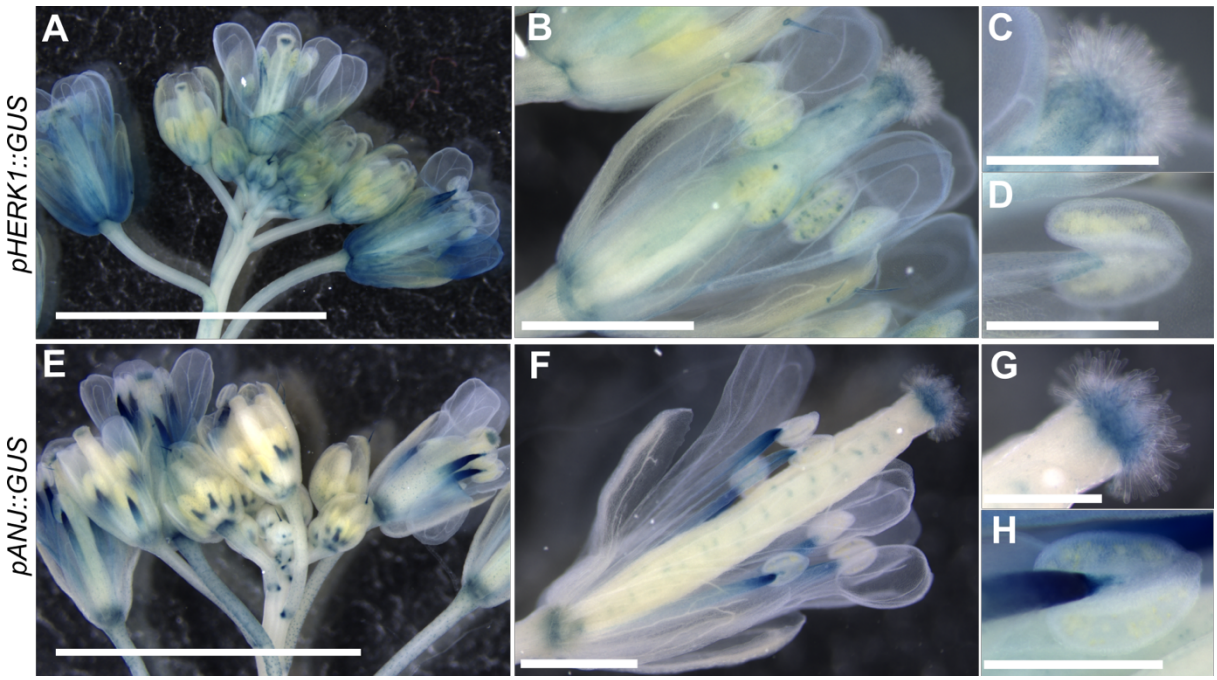

Figure S5. Expression pattern of *HERK1* and *ANJ* in flowers. (A-D) Representative image of the expression pattern in inflorescences and flowers of *HERK1* as shown by *pHERK1::GUS*. Details of a mature stigma and anther are shown in (C) and (D), respectively. GUS activity in at least four T1 lines was examined. (E-H) Representative image of the expression pattern in inflorescences and flowers of *ANJ* as shown by *pANJ::GUS*. Details of a mature stigma and anther are shown in (G) and (H), respectively. GUS activity in at least four T1 lines was examined. Scale bars = 5 mm in (A,E) 1 mm in (B,F); 0.5 mm in (C,D,G,H).

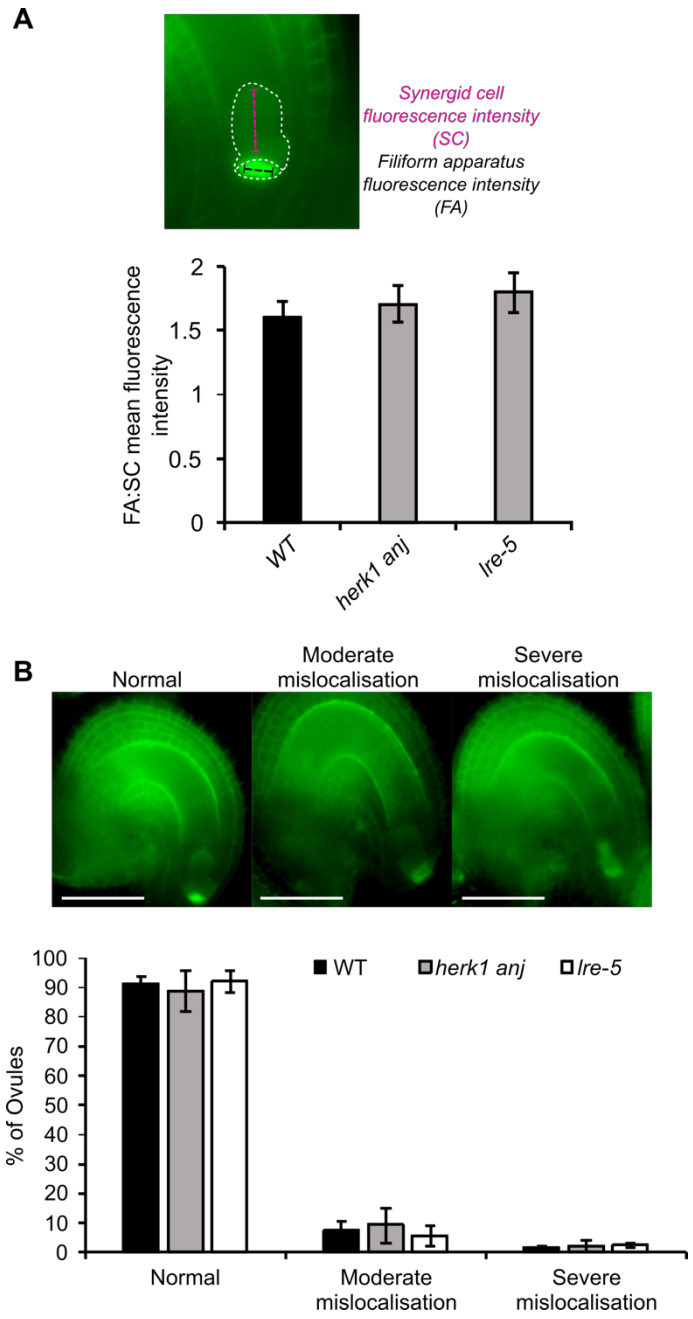

48

49 **Figure S6. Quantification of FER-GFP mislocalisation in the synergid cells of *herk1 anj* and**
50 ***lre-5* ovules.** (A) Ratio between fluorescence intensities at the filiform apparatus (FA) and the
51 synergid cell cytoplasmic region (SC) in mature ovules from wild-type (Col-0), *herk1 anj* and *lre-5*
52 emasculated flowers expressing *pFER::FER-GFP*. Fluorescence profiles for each region of the
53 synergid cells were recorded as exemplified in the upper panel and averaged prior to the ratio
54 calculation (Student's *t* tests, p>0.05). (B) Quantification of moderate and severe mislocalisation
55 defects in the accumulation of FER-GFP at the filiform apparatus in mature ovules from wild-type
56 (Col-0), *herk1 anj* and *lre-5* emasculated flowers expressing *pFER::FER-GFP*. Ovules with clear

57 FER-GFP expression were assigned to one of the three categories presented in the upper panel,
58 as per (Li et al, 2015). Ovules were obtained from three siliques per plant and three plants per line
59 (total of ovules analysed per line >95). No statistically significant differences were detected in
60 Student's *t* test comparisons with wild-type.

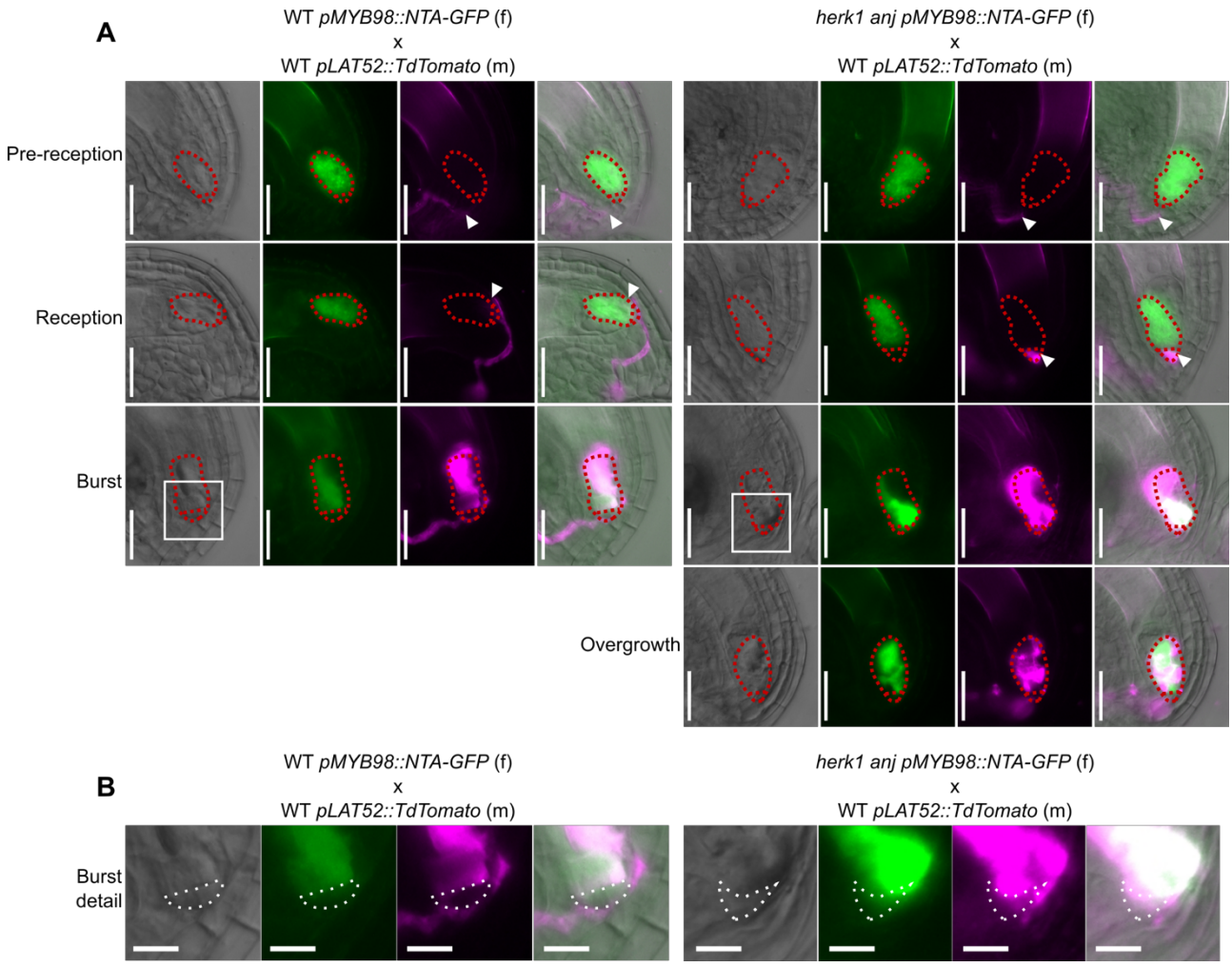

Figure S7. NTA localisation in the synergid cells of WT and *herk1 anj* at different stages of pollen tube reception. (A) DIC images are shown in grey. In green is NTA-GFP fluorescence in ovules expressing *pMYB98::NTA-GFP*. In magenta, TdTomato fluorescence from pollen tubes expressing *pLAT52::TdTomato*. On the right are merged DIC and fluorescence images. Red dotted lines delineate the synergid cells. White arrowheads indicate the pollen tube tip. (B) Detailed images of the filiform apparatus corresponding to the areas highlighted with white squares in (A). White dotted lines delineate the filiform apparatus. Scale bars = 25 µm in (A) and 10 µm in (B).

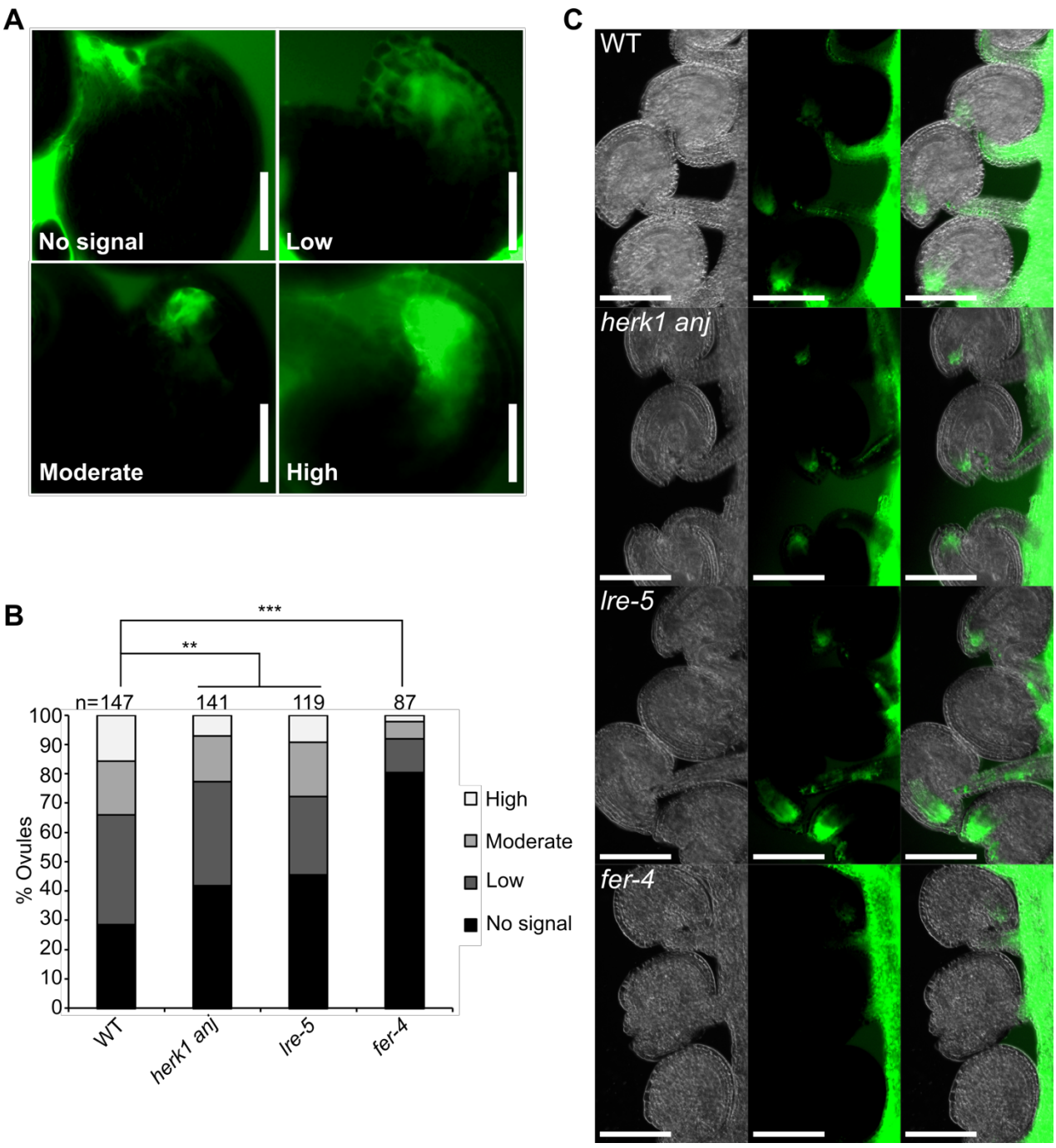

Figure S8. H_2DCF-DA measurements of ROS production in *herk1 anj* ovules. (A) Images of H_2CDF-DA fluorescence in representative ovules corresponding to each category used in the ROS assays presented in this study. Scale bars = 25 µm. (B) Quantification of the H_2CDF-DA staining of ROS in ovules from wild-type, *herk1 anj*, *lre-5*, and *fer-4* plants at 0 HAE. Categories are listed in the legend. Ovules analysed from six siliques per line. ** $p<0.01$; *** $p<0.001$ (χ-square tests). (C) Representative images of H_2CDF-DA staining of ROS in three ovules from wild-type, *herk1 anj*, *lre-5* and *fer-4* plants at 20 hours after emasculation (HAE). Scale bars = 100 µm.

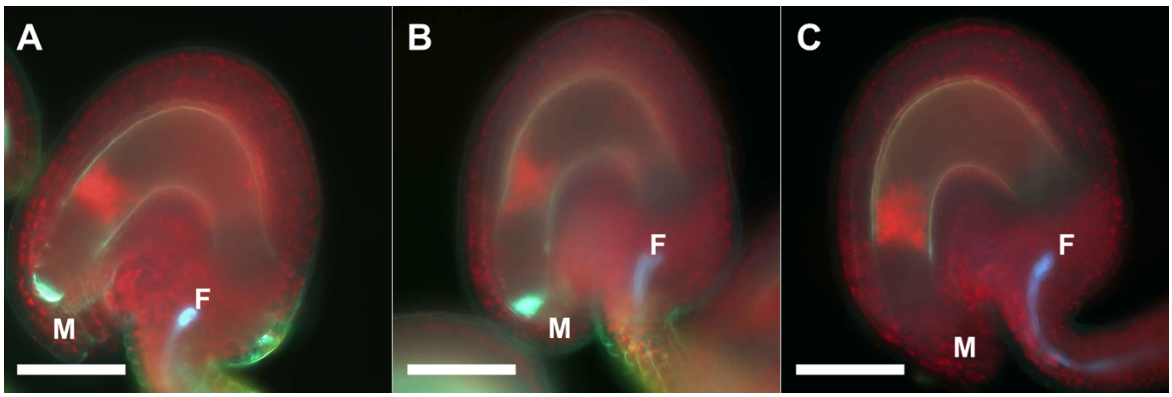

Figure S9. Callose accumulation at the filiform apparatus in *herk1 anj* mutants. (A) Representative image of a mature ovule from a wild-type plant. SR2200 white fluorescence at the filiform apparatus indicates accumulation of callose. (B) Representative image of a mature ovule from a *herk1 anj* plant. SR2200 white fluorescence at the filiform apparatus indicates accumulation of callose. (C) Representative image of the background autofluorescence present in mature ovules. Chlorophyll red autofluorescence can be seen in all cell layers in the ovule. Blue autofluorescence from the xylem lignin within the funiculus can also be observed. Scale bars = 25 μm. M, micropyle. F, funiculus.

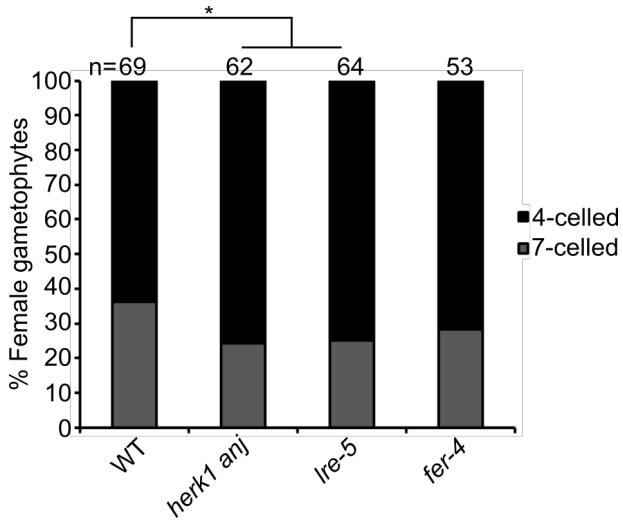

Figure S10. Female gametophyte development at 20 HAE. Female gametophyte developmental stage in ovules from stage 14 flowers at 20 hours after emasculation (HAE) in wild-type, *herk1 anj*, *lre-5* and *fer-4* as assessed by confocal microscopy as per (Christensen et al, 1997). Ovules analysed from five siliques per line. * $p<0.05$ (χ-square tests).

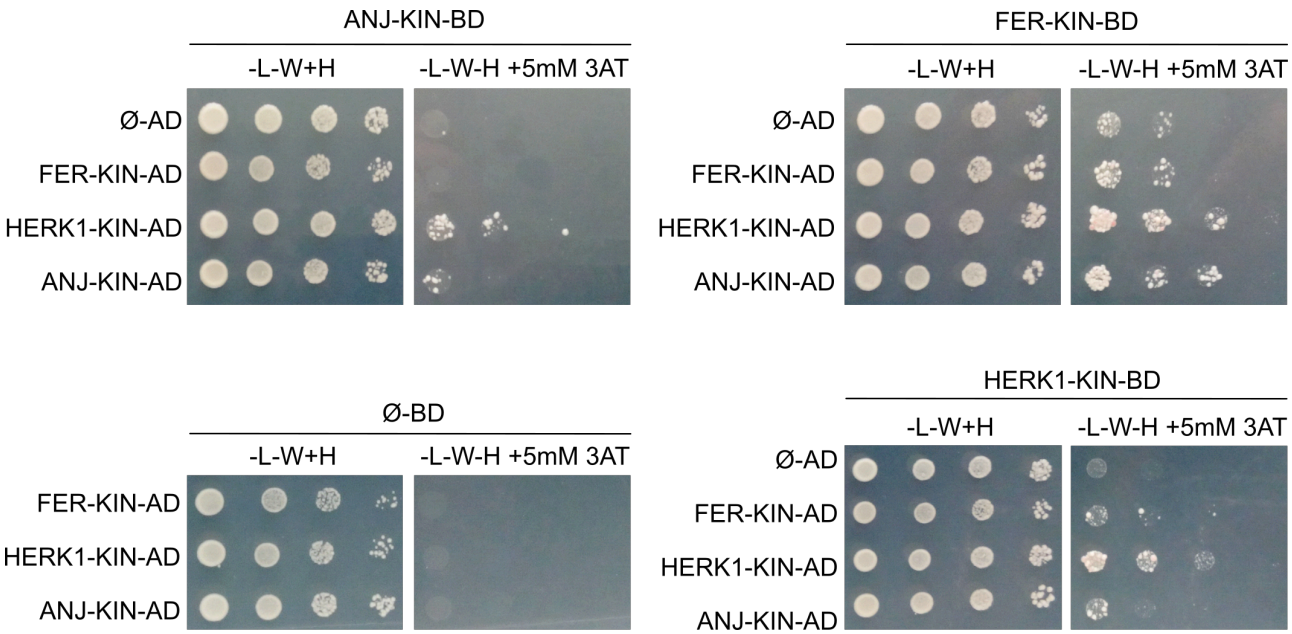

Figure S11. Yeast two hybrid assays between HERK1, ANJ and FER kinase domains. Yeast two hybrid assays with the intracellular kinase domains of HERK1, ANJ and FER (HERK1-KIN, ANJ-KIN and FER-KIN, respectively). Ø represents negative controls where no sequence was cloned into the activating domain (AD) or DNA-binding domain (BD) constructs. -L-W-H, growth medium depleted of leucine (-L), tryptophan (-W) and histidine (-H). Plates were supplemented with 5mM 3-Amino-1,2,4-triazole (3 AT) due to yeast growth autoactivation in several of these constructs.

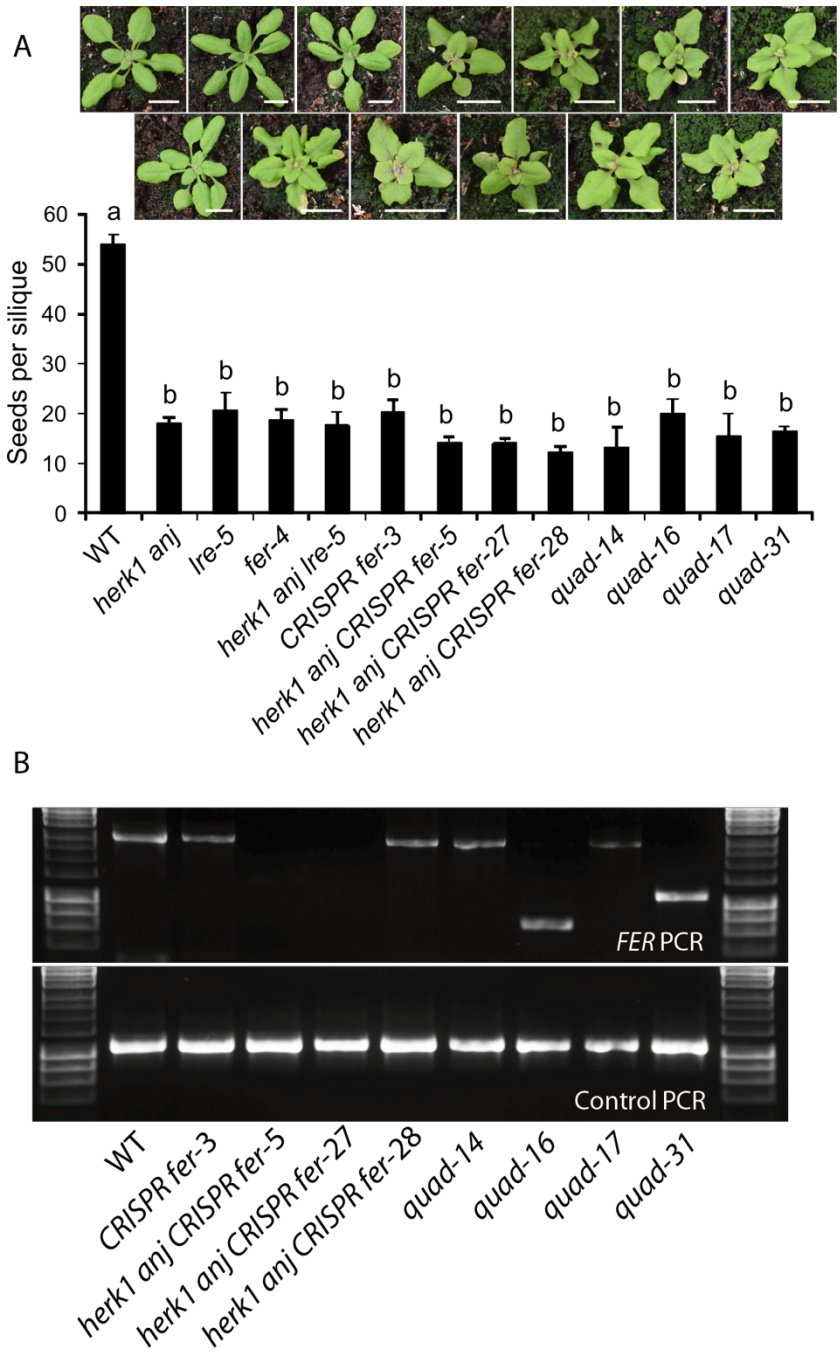

Figure S12. Quantification of seed set in CRISPR-Cas9 *fer* mutants. (A) Developing seeds per silique in wild-type, single, double, triple and quadruple mutants as listed. Quad = *herk1 anj lre-5* CRISPR *fer*. Fully expanded siliques were dissected and photographed using an SLR camera. *n* = 15 (three plants per line and five siliques per plant). Data presented are means ± SD. Letters (a, b) mark statistically significant differences between samples in one-way ANOVA analysis followed by Bonferroni's post-hoc comparison of means ($p<0.05$). Pictures above are of plants at 21 days after sowing. Scale bars = 1 cm. (B) PCR amplification of *FER* and control genomic DNA from wild-

type and CRISPR-Cas9 *fer* mutants. A lack of amplification from *herk1 anj CRISPR fer* lines 5 and 27 is interpreted as deletion of one or both of the primer binding sites.

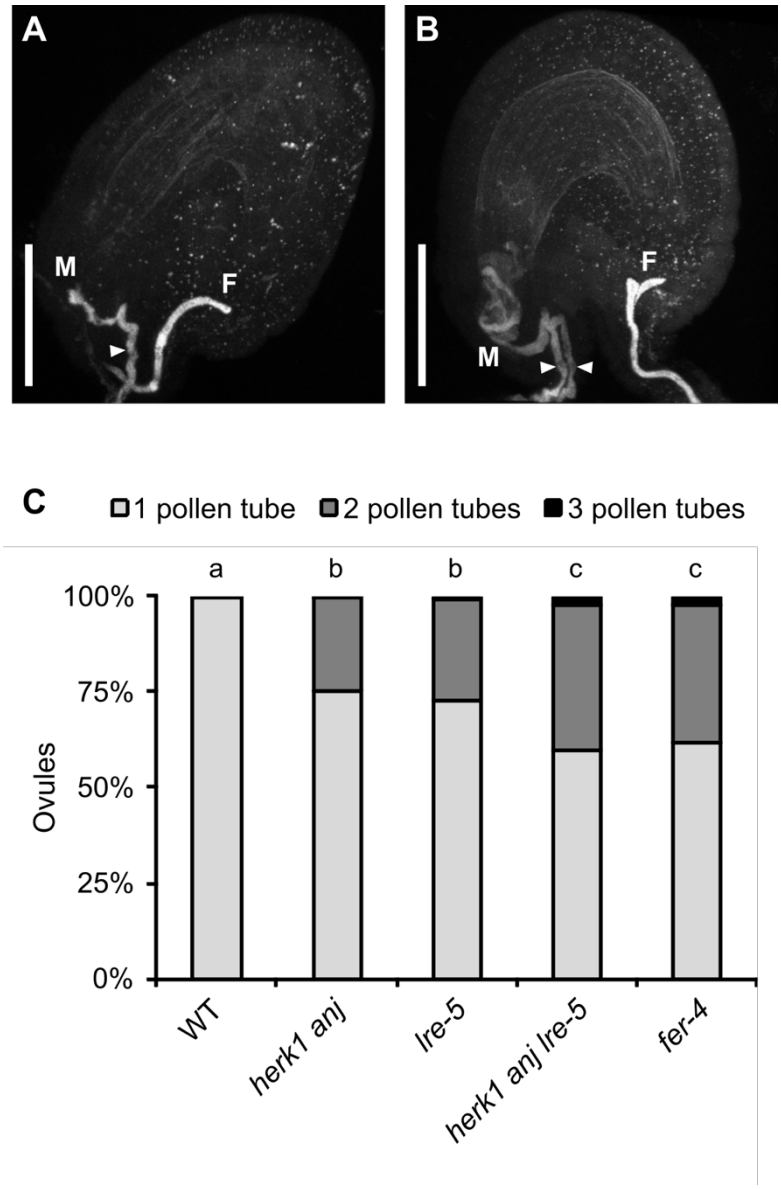

Figure S13. ***herk1 anj*** **ovules attract multiple pollen tubes.** (A) Representative image of a normal pollen tube reception event in a wild-type ovule by confocal microscopy. (B) Representative image of a *herk1 anj* ovule displaying pollen tube overgrowth and multiple pollen tubes in the micropyle. Images are maximum intensity projections from confocal microscopy images across several z-planes of ovules stained with aniline blue. M, micropyle. F, funiculus. White arrowhead, pollen tube. Scale bars = 50 µm. (C) Polytubey quantification in wild-type (Col-0), *herk1 anj*, *lre-5*, *herk1 anj lre-5* and *fer-4* ovules by epifluorescence microscopy following hand pollination at 24h after emasculation. Ovules from 10 to 13 siliques per line were scored for the number of pollen tubes present at the micropyle if fertilised (total fertilised ovules analysed per line >265). Letters (a,

126 b, c) mark statistically significant differences between samples in multiple Fisher's exact test
127 pairwise comparisons ($p<0.001$).

128 **Table S1. List of Arabidopsis lines use in this study.** Sources and NASC stock identifiers are

129 listed where relevant.

Experimental Models: Organisms/Strains		
Arabidopsis thaliana: Col-0	NASC	N1092
Arabidopsis thaliana: herk1-1	NASC	N657488
Arabidopsis thaliana: anj-1	NASC	N654842
Arabidopsis thaliana: fer-4	Prof. A. Cheung (Duan et al, 2014)	NASC ID: N69044
Arabidopsis thaliana: lre-5	Dr. R. Palanivelu (Tsukamoto et al, 2010)	NASC ID: N66102
Arabidopsis thaliana: herk1-1 anj-1	This study	N/A
Arabidopsis thaliana: herk1-1 anj-1 lre-5	This study	N/A
Arabidopsis thaliana: Col-0 CRISPR *fer*	This study	N/A
Arabidopsis thaliana: herk1-1 anj CRISPR *fer*	This study	N/A
Arabidopsis thaliana: Col-0 *herk1 anj lre-5* CRISPR *fer*	This study	N/A
Arabidopsis thaliana: Col-0 *pHERK1::GUS*	This study	N/A
Arabidopsis thaliana: Col-0 *pANJ::GUS*	This study	N/A
Arabidopsis thaliana: Col-0 *pHERK1::H2B-tdTomato*	This study	N/A
Arabidopsis thaliana: Col-0 *pANJ::H2B-tdTomato*	This study	N/A
Arabidopsis thaliana: Col-0 *pHERK1::HERK1*	This study	N/A
Arabidopsis thaliana: Col-0 *pANJ::ANJ-GFP*	This study	N/A

Arabidopsis thaliana: Col-0 *pLRE::LRE-Citrine*	This study	N/A
Arabidopsis thaliana: Col-0 *pMYB98::NTA-GFP*	This study	N/A
Arabidopsis thaliana: Col-0 *pFER::FER-GFP*	This study	N/A
Arabidopsis thaliana: herk1-1 anj-1 pHERK1::HERK1	This study	N/A
Arabidopsis thaliana: herk1-1 anj-1 pANJ::ANJ-GFP	This study	N/A
Arabidopsis thaliana: herk1-1 anj-1 pLRE::LRE-Citrine	This study	N/A
Arabidopsis thaliana: herk1-1 anj-1 pMYB98::NTA-GFP	This study	N/A
Arabidopsis thaliana: herk1-1 anj-1 pFER::FER-GFP	This study	N/A
Arabidopsis thaliana: lre-5 pHERK1::HERK1	This study	N/A
Arabidopsis thaliana: lre-5 pANJ::ANJ-GFP	This study	N/A
Arabidopsis thaliana: lre-5 pLRE::LRE-Citrine	This study	N/A
Arabidopsis thaliana: lre-5 pMYB98::NTA-GFP	This study	N/A
Arabidopsis thaliana: lre-5 pFER::FER-GFP	This study	N/A
Arabidopsis thaliana: Col-0 *pLAT52::TdTomato*	Dr. M. Bayer (unpublished)	N/A

130

131

Table S2. List of primers used for cloning, genotyping PCR or RT-PCR.

Oligonucleotides (5' - 3')	
HERK1 genotyping fw	GTTGCTCGCGGTAGTCTTCT
HERK1 genotyping rv	CTGTCCTGAATTCCGCAAGC
ANJEA genotyping & RT-PCR fw	CTCCTCTGTAGCAAAACCAGGA
ANJEA genotyping & RT-PCR rv	CTCACGTTTACTCCCTCGGG
LRE genotyping fw	AAGCCAGTTTTAGAGTACGAAGA
LRE genotyping rv	TCAAGTCAACACTAACAAAGCAAAAACAGCGG
FER genotyping fw	CGGATCCATGAAGATCACAGAGGGACGATTC
FER genotyping rv	CGCAGATCTAGCACCAAACACACAAAACCC
FER RT-PCR fw	GAGATGCTCCCTCATTGTACC
FER RT-PCR rv	GGCTTACCGCAGACGTAAGC
SALK LB genotyping primer	ATTTTGCCGATTTCGGAAC
GABI LB genotyping primer	GTGGATTGATGTGATATCTCC
pHERK1 fw	TAGGTACCTAGAATGTTTTTCTCAAGTTTTCTTCC
HERK1 rv	TAAGGATCCTCTTCCTTCAGATTTCACCAGTTGTG
pANJ fw	TTAGGTACCTTGTGGAATCATGAAATCGTAGTGT
ANJ rv	TAGGATCCACGTCCCTCAGATTTGATCAGCTGCG
pFER fw	TAGGTACCCGAGTTGTAAAAGGCCTGGC
FER rv	TAAGGATCCACGTCCCTTTGGATTCATGA

HERK1-KD fw	AGAAACGTGAGATCTGCAAACATATTGCTTGACGA
HERK1-KD rv	AGATCTCACGTTTCTGTGAATGACCGGTTTCGAGT
ANJ-KD fw	AGAAACGTCAGATCCGCCAACATATTGCTTGA
ANJ-KD rv	GGATCTGACGTTTCTGTGAATCACGGGTTTCG
pHERK1 pentrdtopo fw	CACCTAGAATGTTTTTCTCAAGTTTTCTTCC
pHERK1 pentrdtopo rv	AACCTGGAAATGGAACAGATC
pANJ pentrdtopo fw	CACCTTGTGGAATCATGAAATCGTAGT
pANJ pentrdtopo rv	TTCACAAAACCTGGAAATTTTAAATAATT
HERK1exJM Y2H (324-406) fw	GGATATTGATCTTAGCACTCTTGTGG
HERK1exJM Y2H (324-406) rv	AACCCGAGATTACTCTTACTGCT
ANJexJM Y2H (324-406) fw	GCTTGATCTGAGCTCTTATTTATCCA
ANJexJM Y2H (324-406) rv	CCACCAACATTCTTCTTAGTGGTTG
LRE Y2H (23-138) fw	GATATCGGATGGTGTGTTTGAATCA
LRE Y2H (23-138) rv	CCGGCGTTTAGGTTATGTGAATAGAG
HERK1 ECD Y2H (24-405) fw	GGATTCACACCTGTGGATAATTAC
HERK1 ECD Y2H (24-405) rv	TTACCCGAGATTACTCTTACTGCT
ANJ ECD Y2H (25-405) fw	TACGTACCAGTGGATAATTACCTC
ANJ ECD (25-405) rv	TTAACCAACATTCTTCTTAGTGGTTG
FER ECD Y2H (28-446) fw	GCTGATTACTCTCCAACAGAGA
FER ECD Y2H (28-446) rv	TTACGTATTGCTTTTCGATTTCCTAG
HERK1 kin Y2H (429-830) fw	GAAGAAGCGGAAACGTGGC

HERK1 kin Y2H (429-830) rv	CCTCTTCCTTCAGATTTCACCAGTTGTG
ANJ kin Y2H (429-830) fw	GAAGAAACGAGGACGAGACC
ANJ kin Y2H (429-830) rv	CCTCCACGTCCCTCAGATTTGATCAGCTGCG
FER kin Y2H (470-895) fw	GGCTTACCGCAGACGTAAGC
FER kin Y2H (470-895) rv	CCACGTCCCTTTGGATTCATGA
FER CRISPR construct 1 Out fw (5' gRNA 1; target FER sequence underlined)	ATATATGGTCTCGATTGTTCTACCCAAACTCGT ACGAGTT
FER CRISPR construct 1 In fw (5' gRNA 1)	TGTTCTACCCAAACTCGTACGAGTTTTAGAGCT AGAAATAGC
FER CRISPR construct 1 In rv (3' gRNA 1)	AACCGAGTCCGTCACATTCCCTTCAATCTCTTA GTCGACTCTAC
FER CRISPR construct 1 Out rv (3' gRNA 1)	ATTATTGGTCTCGAAACCGAGTCCGTCACATTC CCTTCAA
FER CRISPR construct 2 Out fw (5' gRNA 2)	ATATATGGTCTCGATTGAAAAGGAGTATGCGGT GACAGTT
FER CRISPR construct 2 In fw (5' gRNA 2)	TGAAAAGGAGTATGCGGTGACAGTTTTAGAGC TAGAAATAGC
FER CRISPR construct 2 In rv (3' gRNA 2)	AACCGGAAGGCGAGATATCATTCCAATCTCTTA GTCGACTCTAC
FER CRISPR construct 2 Out rv (3' gRNA 2)	ATTATTGGTCTCGAAACCGGAAGGCGAGATAT CATTCCAA
CRISPR-Cas9 *fer* mutant genotyping fw	CATTGACGCGATTCATGTTT
CRISPR-Cas9 *fer* mutant genotyping fw	GATGAAGATCACAGAGGGACG

Control gDNA region for genotyping fw	CTGCCTTACGAGCATTGGTT
Control gDNA region for genotyping rv	TAACGCTTCCCAAGGTGATT

133

134

135 **Table S3. List of plasmids used in the present study and their corresponding sources.**

Recombinant DNA	Reference
pHERK1::HERK1 in pGreen-IIS	This study
pANJ::ANJ-GFP in pGreen-IIS	This study
pFER::FER-GFP in pGreen-IIS	This study
pHERK1:HERK1-KD in pGreen-IIS	This study
pANJ::ANJ-KD-GFP in pGreen-IIS	This study
pHERK1::GUS in pGWB433	This study
pANJ::GUS in pGWB433	This study
pHERK1::H2B-tdTomato in pAH21	This study
pANJ::H2B-tdTomato in pAH21	This study
pFER::HERK1-GFP in pMDC111	Prof. U. Grossniklaus (Kessler et al, 2015)
pMYB98::NTA-GFP in pMDC83	Dr. S. Kessler (Davis et al, 2017)
p35S::HA-LRE in pSK	Dr. C. Li (Li et al, 2015)
p35S::HA-LRE in pMLBart	This study
pLRE::LRE-Citrine in pMDC99	Prof. U. Grossniklaus (Lindner et al, 2015)
pU6-26::FER 5' gRNA 1; pU6-29::FER 3' gRNA 1	This study
pU6-26::FER 5' gRNA 2; pU6-29::FER 3' gRNA 2	This study
pGreen-IIS – Cterm GFP	(Mathieu et al, 2007)
pGWB433	(Nakagawa et al, 2007)

pGADT7	Clontech
pGBKT7	Clontech
pAH21\GW	Dr. M. Butenko
pBEE401E	Prof. D. Goring (Wang et al, 2015)
pCBC-DT1T2	Prof. D. Goring (Wang et al, 2015)

References

Christensen CA, King EJ, Jordan JR, Drews GN (1997) Megagametogenesis in Arabidopsis wild type and the Gf mutant. *Sex Plant Reprod* **10:** 49-64

Davis TC, Jones DS, Dino AJ, Cejda NI, Yuan J, Willoughby AC, Kessler SA (2017) Arabidopsis thaliana MLO genes are expressed in discrete domains during reproductive development. *Plant Reprod* **30:** 185-195

Duan Q, Kita D, Johnson EA, Aggarwal M, Gates L, Wu HM, Cheung AY (2014) Reactive oxygen species mediate pollen tube rupture to release sperm for fertilization in Arabidopsis. *Nat Commun* **5:** 3129

Kessler SA, Lindner H, Jones DS, Grossniklaus U (2015) Functional analysis of related CrRLK1L receptor-like kinases in pollen tube reception. *EMBO Rep* **16:** 107-115

Li C, Yeh FL, Cheung AY, Duan Q, Kita D, Liu MC, Maman J, Luu EJ, Wu BW, Gates L, Jalal M, Kwong A, Carpenter H, Wu HM (2015) Glycosylphosphatidylinositol-anchored proteins as chaperones and co-receptors for FERONIA receptor kinase signaling in Arabidopsis. *Elife* **4**

Lindner H, Kessler SA, Muller LM, Shimosato-Asano H, Boisson-Dernier A, Grossniklaus U (2015) TURAN and EVAN mediate pollen tube reception in Arabidopsis Synergids through protein glycosylation. *PLoS Biol* **13:** e1002139

Mathieu J, Warthmann N, Kuttner F, Schmid M (2007) Export of FT protein from phloem companion cells is sufficient for floral induction in Arabidopsis. *Current Biology* **17:** 1055-1060

Nakagawa T, Suzuki T, Murata S, Nakamura S, Hino T, Maeo K, Tabata R, Kawai T, Tanaka K, Niwa Y, Watanabe Y, Nakamura K, Kimura T, Ishiguro S (2007) Improved Gateway Binary Vectors: High-Performance Vectors for Creation of Fusion Constructs in Transgenic Analysis of Plants. *Bioscience, Biotechnology, and Biochemistry* **71:** 2095-2100

Tsukamoto T, Qin Y, Huang YD, Dunatunga D, Palanivelu R (2010) A role for LORELEI, a putative glycosylphosphatidylinositol-anchored protein, in Arabidopsis thaliana double fertilization and early seed development. *Plant Journal* **62:** 571-588

Wang ZP, Xing HL, Dong L, Zhang HY, Han CY, Wang XC, Chen QJ (2015) Egg cell-specific promoter-controlled CRISPR/Cas9 efficiently generates homozygous mutants for multiple target genes in Arabidopsis in a single generation. *Genome Biol* **16:** 144